HHS Public Access

Author manuscript

Free Radic Res. Author manuscript; available in PMC 2023 April 15.

Published in final edited form as:

Free Radic Res. 2022 February ; 56(2): 163–172. doi:10.1080/10715762.2022.2061967.

Hypoxia Induces Proliferation via NOX4-Mediated Oxidative Stress and TGF-β3 Signaling in Uterine Leiomyoma Cells

Mariko Miyashita-Ishiwata, MD, PhD[1], **Malak El Sabeh, MD**[1], **Lauren D Reschke, MD**[1], **Sadia Afrin, PhD**[1], **Mostafa A Borahay, MD, PhD**[1,*]

[1]Department of Gynecology and Obstetrics, Johns Hopkins University, Baltimore, MD, USA, Address: 4940 Eastern Ave, Baltimore, MD, USA 21224-2780

Abstract

Uterine leiomyomas, the most common tumors of the female reproductive system, are known to have a hypoxic microenvironment. However, the role of such environment in leiomyoma pathobiology remains unknown. The objective was to determine the effects of hypoxia on leiomyoma cells, and the mechanisms. We found that hypoxia induces proliferation and inhibits apoptosis in human leiomyoma cells. This pro-proliferative effect was accompanied by an increase in reactive oxygen species (ROS) generation and the expression of NADPH oxidase 4 (NOX4). The specific NOX4 inhibitor GLX351322 abrogated this hypoxia-induced ROS generation, cellular proliferation, and apoptosis inhibition. To further investigate the mechanism of NOX4-mediated proliferation, we treated leiomyoma cells grown in normoxia with media from leiomyoma cells cultured under hypoxia. This resulted in increased ROS generation and NOX4 expression, suggesting the hypoxia-induced effects are mediated by an autocrine mechanism. We worked to identify the nature of this autocrine factor. We found that the expression of TGF-β3 and its downstream signaling target pSmad3, are increased in hypoxic leiomyoma cells. To examine the hypothesis that TGF-β3 is, at least, a part of this autocrine mechanism, we treated hypoxic leiomyoma cells with the HIF-1α inhibitor KC7F2 which we discovered to ameliorate the hypoxia-induced TGF-β3 expression. Furthermore, pharmacologic inhibition with the TGF-β/Smad inhibitor SB431542 reduced hypoxia-induced NOX4 expression and ROS generation and attenuated cell proliferation. Thus, we have identified a novel mechanism by which hypoxia induces proliferation in leiomyoma cells. This finding adds to our understanding of leiomyoma pathobiology and can help in identifying new therapeutic targets.

GRAPHICAL ABSTRACT.

[*]**Correspondence address:** Department of Gynecology & Obstetrics, Johns Hopkins University School of Medicine, 720 Rutland Ave, Baltimore, MD, 21205, USA, mboraha1@jhmi.edu, .

Disclosure of interest

The authors report no conflict of interest.

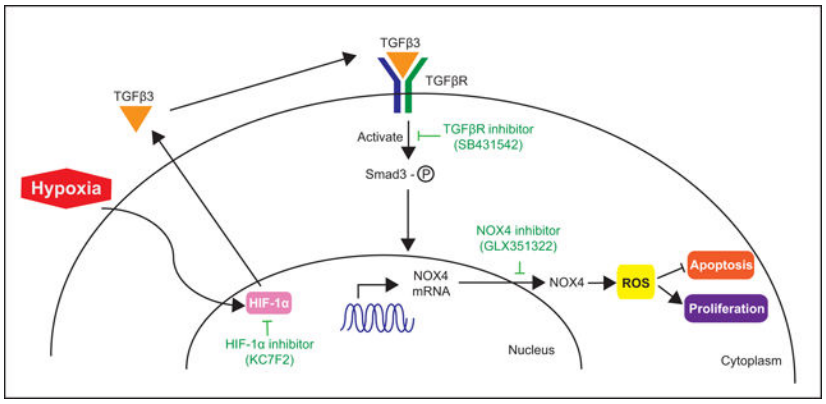

A cartoon illustrating the mechanism by which hypoxia induces NOX4-mediated leiomyoma cell proliferation via ROS generation and TGF-β3 pathway. HIF-1α, hypoxia inducible factor 1 alpha; TGF-β3, transforming growth factor beta 3; TGFβR, transforming growth factor beta receptor; NOX4, nicotinamide adenine dinucleotide phosphate (NADPH) oxidase 4; ROS, reactive oxygen species.

Keywords

Leiomyoma; hypoxia; oxidative stress; NOX4; TGF-β3; ROS

INTRODUCTION

Uterine leiomyomas (fibroids) are the most common tumors of the female reproductive system. They cause significant medical problems including heavy menstrual bleeding, anemia, pelvic pain, and subfertility (Lewis et al., 2018). Despite their high prevalence (up to 70% of women by the age of 50) and significant burden, their exact pathogenesis is not well understood, and, therefore, effective management options are limited (Baird et al., 2003).

Leiomyomas are known to grow in a hypoxic microenvironment (Mayer et al., 2008). Hypoxia triggers a number of critical adaptations that enable cell survival, including altered metabolism (Fruehauf and Meyskens, 2007). Evidence suggests that hypoxia induces reactive oxygen species (ROS) generation and oxidative stress (Clanton, 2007). However, the interplay between hypoxia, ROS and other pathways driving leiomyoma growth is not clearly understood.

Nicotinamide adenine dinucleotide phosphate (NADPH) oxidase (NOX), a family of isoenzymes, is one of the major sources of ROS (Knock, 2019). Leiomyomas appear to have an altered pro-oxidant enzyme system. For example, NOX4, one of ROS sources, was found to be overexpressed in human leiomyoma compared to myometrial tissues (Fletcher et al., 2017; Fletcher et al., 2014). However, its regulatory mechanisms in leiomyomas are not clearly known.

TGF-β3 is a member of the transforming growth factor superfamily and is overexpressed 3- to 5-fold in uterine leiomyomas compared to myometrium (Luo et al., 2005; Malik and Catherino, 2007). TGF-β3 is a key regulator of the deposition of many extracellular matrix (ECM) proteins and contributes to leiomyoma growth (Arici and Sozen, 2000; Borahay et al., 2015a; Lee and Nowak, 2001; Massagué and Wotton, 2000). In human bronchial epithelial cells, NOX4 was shown to be regulated by TGF-β3 (Zhang et al., 2019). However, it is unknown if such a mechanism is also present in leiomyoma.

The hypothesis of this study is that hypoxia stimulates leiomyoma growth by inducing oxidative stress. Specifically, we hypothesize that hypoxia inducible factor-1 alpha (HIF-1α) increases the expression of TGF-β3, which in turn stimulates NOX4 expression leading to increased ROS generation which increases cellular proliferation and inhibits apoptosis. Thus, in this work, we examined the role of NOX4 in ROS-mediated leiomyoma growth and investigated the mechanism by which NOX4 is induced under hypoxia.

MATERIALS AND METHODS

Isolation and culture of primary leiomyoma and myometrial cells

Primary leiomyoma and myometrial cells were isolated as previously described (Afrin et al., 2021; Afrin et al., 2020; Borahay et al., 2014; El Sabeh et al., 2021). Briefly, cells were isolated from patients who underwent hysterectomy at the Johns Hopkins University Hospital. The Institutional Review Board of the Johns Hopkins University reviewed and approved the study, and informed consents were obtained from patients. Tissues were brought to the laboratory immediately after surgery and washed several times with a Hanks' Balanced Salt Solution (HBSS, Thermo Fisher Scientific, Waltham, MA) without calcium or magnesium. The tissues were manually cut into small pieces (1–2 mm^3) and incubated in sterile HBSS (without calcium, or magnesium) with collagenase (Worthington, Lakewood, NJ), deoxyribonuclease (DNase, Sigma-Aldrich, St. Louis, MO), antibiotic-antimycotic mixture (Thermo Fisher Scientific), and HEPES buffer solution (Thermo Fisher Scientific) at 37ºC on a shaker for 4–8 hours. The digest was filtered through a 100-μm filter and a 40-μm filter and cultured in Dulbecco's Modified Eagle Medium/Nutrient Mixture F12 (DMEM/F-12) (Thermo Fisher Scientific) medium supplemented with HEPES, L-glutamine, 10% FBS, and 1% antibiotic-antimycotic.

Preparation of conditioned media

Primary leiomyoma cells were preincubated without serum for 24h. The cells were then incubated in 2% or 21% O_2 at 37ºC with 10% FBS. After 24h, the media were removed, and the volume of the media was noted. The conditioned media were either used immediately or stored at −80ºC for later use.

Drug treatments

Cells were seeded at a concentration of 0.6×10^5 cells/ml until 60–70% confluence. Cells were treated with GLX351322 (specific NOX4 inhibitor, 40μM, MedChemExpress, Monmouth Junction, NJ), KC7F2 (HIF-1α translational inhibitor, 20μM, Selleck Chemicals, Houston, TX), TGF-β3 (10ng/ml, Sigma-Aldrich, St. Louis, MO) and SB431542 (TGF-β

type1 receptor/Smad inhibitor, 10 μM, Cayman chemical, Ann Arbor, MI) and incubated for an additional 24 or 48 hours. Control cells were incubated with an equal amount of Dimethyl sulfoxide (DMSO, Corning, Glendale, AZ).

RNA extraction and quantitative real-time polymerase chain reaction

Cells were plated in a 12-well plate at a concentration of 1.2×10^5 cells/well and maintained with complete DMEM/F-12 media until 60–70% confluence. The total RNA content was extracted by using an Rneasy Mini Kit (QIAGEN, Gaithersburg, MD) as per manufacturer's instructions. RNA concentration and purity were measured using the NanoVue Plus (Biochrom US Inc, Holliston, MA). Reverse transcription was performed using the iScript cDNA Synthesis Kit (Bio-Rad, Hercules, CA) in a Bio-Rad Thermocycler according to the manufacturer's instructions. One microgram of total RNA from each sample was reverse transcribed in 20μL reaction volume to complementary DNA (cDNA). Quantitative real-time polymerase chain reaction (qRT-PCR) was performed using the LightCycler 96 System (Roche Diagnostics, Mannheim, Germany) and FastStart Essential DNA Green Master (Roche Diagnostics) according to the manufacturer's protocol. An equal amount of cDNA of each sample was added to the master mix containing appropriate primer sets in a 10-μL reaction volume. All experiments were performed in duplicates and repeated at least 3 times. *RPLP0* was amplified under the same qRT-PCR conditions for normalizing the quantitative data. The *NOX4* primers (sense, 5'-AGTCCTTCCGTTGGTTTG-3'; antisense, 5'-AAAGTTTCCACCGAGGAC −3') were chosen to amplify a 186-bp fragment. The *RPLP0* primers (sense, 5'-GCGACCTGGAAGTCCAACT-3'; antisense, 5'-GGTCCTCCTTGGTGAACAC-3') were chosen to amplify a 265-bp fragment. The relative mRNA expression was calculated using the ΔΔCT method and is presented as fold increase relative to control levels expressed as 1.00.

Protein extraction and western blot analysis

Cells were cultured in a 60-mm dish (5×10^5 cells/dish) with a complete DMEM/F-12 media, until they reached 60–70% confluence. Cells were lysed by adding Laemmli sample buffer (Bio-Rad, Hercules, California) directly to the culture dishes to solubilize the cells. After that, lysates were sonicated and boiled at 99ºC for 5 minutes. For western blotting, protein lysates were resolved in 4%−12% Bis-Tris protein gradient gels (Thermo Fisher Scientific) for electrophoresis and then transferred onto a nitrocellulose membrane (Thermo Fisher Scientific). The membrane was blocked with 5% nonfat milk in Tris-buffered saline with 0.1% Tween-20 (TBST, Thermo Fisher Scientific) for 1 hour at room temperature. Membranes were incubated with specific primary antibodies: anti-HIF-1α (Cell Signaling Technology [CST], Danvers, MA), anti-NOX4 (Abcam, Cambridge, MA), anti-TGF-β3 (Invitrogen, Carlsbad, CA), anti-Smad2/3 (CST), and anti-phospho Smad3 (CST) overnight at 4ºC. Membranes were incubated with appropriate horseradish peroxidase (HRP)-conjugated secondary antibodies (GE Healthcare, Chicago, IL) for 1 hour at room temperature. Immunolabeled proteins were identified using a SuperSignal West Pico PLUS Chemiluminescent Substrate (Thermo Fisher Scientific), and specific protein bands were visualized using Azure Imager c300 (Azure Biosystems, Dublin, CA). The band intensity was quantified using NIH ImageJ software and normalized against corresponding anti-β-actin antibody (CST); normalized values were used to create final graphs.

Enzyme-linked immunosorbent assay

After treatment, the different conditioned media were collected, centrifuged, and stored at −80ºC. The media was shipped to Eve Technologies Corporation (Calgary, AB, Canada) and assayed. TGF-β3 concentrations were measured using Multiplex Immunoassay analyzed with BioPlex 200. The limit of sensitivity of ELISA was 2.2 pg/mL. The intra- and inter- assay coefficients of variation (CV) were 6.3% CV and 8.1% CV. There was no cross-reactivity or interference.

MTT (3-(4,5-Dimethylthiazol-2-yl)-2,5-Diphenyltetrazolium Bromide) assay

Using 96-well plates, 3000 cells were seeded per well with a complete DMEM/F-12 media. One day after seeding, cells were treated. 20μl of 12μM MTT (Thermo Fisher Scientific) solution was added to each well, and cells were incubated for 3 hours. The media was removed, and 100 ul/well DMSO was added. The absorbance at 570 nm was monitored by a microplate reader (CLARIOstar, Cary, NC). Proliferation was normalized relative to the absorbance of cell cultures under normoxic condition. Experiments were performed in quintuplicate.

ROS measurements

Changes in intracellular ROS levels were determined using the fluorogenic probe 5-(and-6)-chloromethyl-2′,7′-dichlorodihydrofluorescein diacetate acetyl ester (CM-H2DCF-DA; Invitrogen, Eugene, OR). Briefly, one day after seeding in a 96-well plate, cells were treated. 5 μM CM-H2DCF-DA was added to each well, and cells were incubated at 37°C for 30 min. Cells were then washed with HBSS. Empty wells without plated cells were used as a negative control. Changes in DCF fluorescence were recorded on a microplate reader (CLARIOstar) at 485 nm excitation and 528 nm emission. Results are expressed as fold change or arbitrarily in fluorescence units (FU). Experiments were performed in quintuplicate.

Caspase-3 assay

Caspase-3 activity was measured with a quantitative fluorometric assay as previously described (Borahay et al., 2015c). In brief, cells were seeded in 6-cm dishes, and cell lysates were obtained. Cell lysates that contained equal amounts of proteins were loaded in a 96-well plate in addition to a reaction mixture that contained Z-DEVD-R110 (caspase-3 substrate, Cayman Chemical). Caspase-3 activity was measured fluorometrically over a period of 60 minutes.

Statistical analysis

All experiments were done in duplicates and repeated at least three independent times. Data were expressed as mean ± standard error of the mean (SEM). An unpaired 2-tailed Student's t-test was used to compare data with control using JMP software (SAS Institute Inc, Cary, NC). $P<0.05$ was considered statistically significant.

RESULTS

Hypoxia induces proliferation and ROS generation and inhibits apoptosis in leiomyoma cells

To assess the effects of hypoxia on the proliferation and apoptosis, primary human leiomyoma cells were cultured under hypoxic (2% O_2) or normoxic conditions for 24 hours. MTT assay showed that leiomyoma cells proliferated 31% more under hypoxic condition (n=8, $P<0.05$, Figure 1A). In addition, a fluorometric caspase-3 activity assay demonstrated a significant decrease of apoptosis by 26% under hypoxic condition (n=5, $P<0.05$, Figure 1B). To investigate the effects of hypoxia on ROS levels, we used the fluorogenic probe CM-H2DCF-DA. As demonstrated in Figure 1C, 24-hour exposure to hypoxia significantly increased ROS generation by leiomyoma cells (n=7, $P<0.005$).

Hypoxia induces NOX4 expression

As NOX4 is known to be a major source of ROS, we sought to confirm its expression in leiomyoma cells and compare it to myometrial cells. We found that NOX4 mRNA and protein expressions were significantly higher in leiomyoma cells compared to myometrial cells (Supplementary figure 1), validating previous reports (Fletcher et al., 2014). To examine our hypothesis that hypoxia induces NOX4 expression in leiomyoma, cells were cultured under hypoxic condition for 24 hours. Hypoxic condition significantly increased NOX4 mRNA expression by 239% (n=5, $P<0.05$, Figure 2A) and protein expression by 43% (n=4, $P<0.05$, Figure 2B).

NOX4 mediates hypoxia-induced ROS generation and proliferation and apoptosis inhibition in leiomyoma cells

To examine the hypothesis that NOX4 mediates hypoxia-induced ROS generation, cellular proliferation and apoptosis inhibition, we used the specific NOX4 inhibitor GLX351322 (40μM for 24 hours). GLX351322 significantly attenuated hypoxia-induced ROS generation (n=4, Figure 3A), cell proliferation (n=4, Figure 3B) and apoptosis inhibition (n=3, Figure 3C). These results indicate that the increase in NOX4 expression in hypoxic leiomyoma cells contributes to cell proliferation and apoptosis inhibition.

Autocrine factors mediate hypoxic ROS generation and NOX4 expression

To determine whether hypoxia directly increases ROS generation in leiomyoma cells or acts through indirect autocrine production of undefined mediators, culture media were removed from cells exposed to 2% O_2 for 24 h and were added to normoxic cells. 24 hours later, ROS generation was assessed. Hypoxia-conditioned media increased ROS generation by 23%, compared with media from normoxic cells (n=4, $P<0.05$, Figure 4A). NOX4 protein expression in leiomyoma cells treated with hypoxia-conditioned media was significantly increased (n=4, $P<0.05$, Figure 4B). This indicates that hypoxic leiomyoma cells produce soluble mediators that cause ROS generation.

Hypoxia induces TGF-β3 and Smad3 phosphorylation

Hypoxia is known to upregulate of TGF-βs in some cell types (Moon et al., 2012; Nishi et al., 2004; Zhou et al., 2009). Thus, we hypothesized that TGF-β3 is at least a component of the autocrine factors mediating hypoxia-induced ROS generation, cellular proliferation and apoptosis inhibition. Therefore, to explore whether TGF-β3, a well-known profibrotic cytokine, is induced by hypoxia in leiomyoma, cells were cultured under hypoxic condition for 24 hours. We found that hypoxia significantly increased TGF-β3 protein expression, and this increase was attenuated by the HIF-1α inhibitor KC7F2 (20 μM) (n=4, Figure 4C). We also found that the level of TGF-β3 as measured by ELISA in the culture media of the hypoxic leiomyoma cells was higher than those from normoxic cells (n=3, $P<0.05$, Figure 4D). The rate of Smad3, a downstream signaling target of TGF-β3, phosphorylation was significantly higher in hypoxic leiomyoma cells compared to those in normoxic conditions and attenuated by KC7F2 (n=4, $P<0.05$, Figure 4E). Hypoxia-induced NOX4 expression was also attenuated by KC7F2 (n=3, $P<0.05$, Figure 4F). These results indicate that hypoxia induces HIF-1α and activates TGF-β3/Smad3/NOX4 pathway in leiomyoma cells.

TGF-β3 induces NOX4 expression, ROS generation, cellular proliferation and inhibits apoptosis in leiomyoma cells

To determine whether TGF-β3 induces NOX4 expression, ROS generation and cellular proliferation, and inhibits apoptosis in leiomyoma, cells were treated with TGF-β3 (10 ng/ml). Treatment with TGF-β3 for 24 and 48 hours induced phosphorylation of Smad3 with decreased expression of total Smad3 (n=4, $P<0.05$, Figure 5A). TGF-β3 also significantly increased NOX4 expressions as measured by real-time PCR and western blotting (Figure 5B and 5C). Moreover, TGF-β3 increased ROS generation when cells were treated for 48 hours (n=3, $P<0.005$, Figure 5D). TGF-β3 treatment also increased leiomyoma cell proliferation and decreased apoptosis (Figure 5E and 5F).

TGF-β3 mediates NOX4-dependent hypoxia-induced proliferation, ROS generation and apoptosis inhibition in leiomyoma cells

The findings related above suggest that hypoxia may increase NOX4-mediated leiomyoma cell proliferation via the autocrine production of TGF-β3. To examine this hypothesis, leiomyoma cells were pretreated with and without the TGF-β type1 receptor/Smad inhibitor SB431542 (10 μM) and then incubated under normoxia and hypoxia. NOX4 expressions with real-time PCR and western blotting were significantly attenuated by pretreatment with SB431542 under hypoxia (Figure 6A and 6B). SB431542 significantly reduced the hypoxia induced Smad3 phosphorylation (Figure 6C). SB431542 significantly attenuated hypoxia-induced ROS generation (n=3, Figure 6D), cell proliferation (n=3, Figure 6E) and apoptosis inhibition (n=3, Figure 6F). These results indicate that TGF-β3 is upstream of NOX4-induced ROS generation and cell growth.

DISCUSSION

The results of this study show that leiomyoma cellular proliferation and apoptosis are regulated through NOX4-generated ROS under hypoxic condition. By pharmacologically

inhibiting HIF-1α, TGF-β/Smad, and NOX4, it seems that hypoxia induces cellular proliferation via the HIF-1α/TGF-β3/Smad3/NOX4 signaling cascade (Graphical abstract).

TGF-βs have three isoforms, and TGF-β3 is the isoform most involved in ECM deposition in leiomyoma cells (Malik and Catherino, 2007). TGF-β3 is thought to play a central role in the early transformational events of normal myometrium to the leiomyomatous phenotype and that elevated TGF-β3 contribute to the leiomyoma growth (Halder et al., 2011). In this study, we demonstrated that TGF-β3 increased leiomyoma cell proliferation and this is the first study to report that hypoxia induces TGF-β3 expression in human leiomyoma cells.

TGF-β3 is known to be regulated by HIF-1 (Chen and Khalil, 2017), a transcription factor that regulates cellular adaptations to hypoxia. Under hypoxic condition, HIF-1α is upregulated, and the HIF-1 complex binds to the hypoxia-response element (HRE) of the gene promoter for transactivation. We demonstrated that the increase in TGF-β3 protein expression by hypoxic leiomyoma cells was suppressed by HIF-1α inhibitor. This result suggests that hypoxia transactivates the TGF-β3 promoter activity and enhances endogenous TGF-β3 expression via HIF-1 signaling pathway. Smad3 is known to be activated by TGF-β3 to regulate cellular proliferation and ECM formation (Borahay et al., 2015b). Phosphorylated isoforms of Smad3 are overexpressed in leiomyoma tissues (Norian et al., 2009; Salama et al., 2012). In this study, we found that phosphorylation of Smad3 was induced by TGF-β3. The application of TGF-β type1 receptor/Smad inhibitor to hypoxic cells attenuated phosphorylated Smad3, NOX4 expression and ROS generation, suggesting the mechanism whereby hypoxia causes NOX4-mediated leiomyoma cell proliferation is dependent on an autocrine activity of TGF-β3, and Smad3 activation.

There is evidence that the TGF-β pathway regulates HIF-1α stabilization and therefore its activity (Mallikarjuna et al., 2019; McMahon et al., 2006). Therefore, it appears that there may be a cross talk between HIF-1 and TGF-β signaling forming a closed loop that may amplify the biological response to hypoxia. This can potentially increase the therapeutic potential of this pathway. Future studies can examine this potential in vivo using our previously published leiomyoma animal model (Borahay et al., 2015c; Borahay et al., 2021).

Potential therapeutic implications

In summary, our study shows that hypoxia induces leiomyoma cells proliferation by a NOX4-mediated mechanism. The hypoxic expression of NOX4 requires the sequential autocrine production of TGF-β3 as well as Smad3 signaling. Therefore, the components of this signaling cascade can be therapeutic targets in leiomyoma therapy.

Supplementary Material

Refer to Web version on PubMed Central for supplementary material.

Funding

This work was supported, in part, by National Institutes of Health grant 1R01HD094380 to MA. B.

References

Afrin S, El Sabeh M, Islam MS, Miyashita-Ishiwata M, Malik M, Catherino WH, Akimzhanov AM, Boehning D, Yang Q, Al-Hendy A, Segars JH, Borahay MA, 2021. Simvastatin modulates estrogen signaling in uterine leiomyoma via regulating receptor palmitoylation, trafficking and degradation. Pharmacological research : the official journal of the Italian Pharmacological Society 172, 105856.10.1016/j.phrs.2021.105856.

Afrin S, Islam MS, Patzkowsky K, Malik M, Catherino WH, Segars JH, Borahay MA, 2020. Simvastatin ameliorates altered mechanotransduction in uterine leiomyoma cells. Am J Obstet Gynecol 223(5), 733.e731–733.e714.10.1016/j.ajog.2020.05.012.

Arici A, Sozen I, 2000. Transforming growth factor-beta3 is expressed at high levels in leiomyoma where it stimulates fibronectin expression and cell proliferation. Fertil Steril 73(5), 1006–1011.10.1016/s0015-0282(00)00418-0. [PubMed: 10785229]

Baird DD, Dunson DB, Hill MC, Cousins D, Schectman JM, 2003. High cumulative incidence of uterine leiomyoma in black and white women: ultrasound evidence. Am J Obstet Gynecol 188(1), 100–107.10.1067/mob.2003.99. [PubMed: 12548202]

Borahay MA, Al-Hendy A, Kilic GS, Boehning D, 2015a. Signaling Pathways in Leiomyoma: Understanding Pathobiology and Implications for Therapy. Molecular medicine.10.2119/molmed.2014.00053.

Borahay MA, Al-Hendy A, Kilic GS, Boehning D, 2015b. Signaling Pathways in Leiomyoma: Understanding Pathobiology and Implications for Therapy. Mol Med 21(1), 242–256.10.2119/molmed.2014.00053. [PubMed: 25879625]

Borahay MA, Kilic GS, Yallampalli C, Snyder RR, Hankins GD, Al-Hendy A, Boehning D, 2014. Simvastatin potently induces calcium-dependent apoptosis of human leiomyoma cells. J Biol Chem 289(51), 35075–35086.10.1074/jbc.M114.583575. [PubMed: 25359773]

Borahay MA, Vincent K, Motamedi M, Sbrana E, Kilic GS, Al-Hendy A, Boehning D, 2015c. Novel effects of simvastatin on uterine fibroid tumors: in vitro and patient-derived xenograft mouse model study. Am J Obstet Gynecol 213(2), 196.e191–198.10.1016/j.ajog.2015.03.055.

Borahay MA, Vincent KL, Motamedi M, Tekedereli I, Salama SA, Ozpolat B, Kilic GS, 2021. Liposomal 2-Methoxyestradiol Nanoparticles for Treatment of Uterine Leiomyoma in a Patient-Derived Xenograft Mouse Model. Reprod Sci 28(1), 271–277.10.1007/s43032-020-00248-w. [PubMed: 32632769]

Chen J, Khalil RA, 2017. Matrix Metalloproteinases in Normal Pregnancy and Preeclampsia. Prog Mol Biol Transl Sci 148, 87–165.10.1016/bs.pmbts.2017.04.001. [PubMed: 28662830]

Clanton TL, 2007. Hypoxia-induced reactive oxygen species formation in skeletal muscle. J Appl Physiol (1985) 102(6), 2379–2388.10.1152/japplphysiol.01298.2006. [PubMed: 17289907]

El Sabeh M, Saha SK, Afrin S, Borahay MA, 2021. Simvastatin inhibits Wnt/beta-catenin pathway in uterine leiomyoma. Endocrinology.10.1210/endocr/bqab211.

Fletcher NM, Abusamaan MS, Memaj I, Saed MG, Al-Hendy A, Diamond MP, Saed GM, 2017. Oxidative stress: a key regulator of leiomyoma cell survival. Fertil Steril 107(6), 1387–1394.e1381.10.1016/j.fertnstert.2017.04.015. [PubMed: 28483502]

Fletcher NM, Saed MG, Abuanzeh S, Abu-Soud HM, Al-Hendy A, Diamond MP, Saed GM, 2014. Nicotinamide adenine dinucleotide phosphate oxidase is differentially regulated in normal myometrium versus leiomyoma. Reprod Sci 21(9), 1145–1152.10.1177/1933719114522552. [PubMed: 24520084]

Fruehauf JP, Meyskens FL Jr., 2007. Reactive oxygen species: a breath of life or death? Clin Cancer Res 13(3), 789–794.10.1158/1078-0432.Ccr-06-2082. [PubMed: 17289868]

Halder SK, Goodwin JS, Al-Hendy A, 2011. 1,25-Dihydroxyvitamin D3 reduces TGF-beta3-induced fibrosis-related gene expression in human uterine leiomyoma cells. J Clin Endocrinol Metab 96(4), E754–762.10.1210/jc.2010-2131. [PubMed: 21289245]

Knock GA, 2019. NADPH oxidase in the vasculature: Expression, regulation and signalling pathways; role in normal cardiovascular physiology and its dysregulation in hypertension. Free Radic Biol Med 145, 385–427.10.1016/j.freeradbiomed.2019.09.029. [PubMed: 31585207]

Lee BS, Nowak RA, 2001. Human leiomyoma smooth muscle cells show increased expression of transforming growth factor-beta 3 (TGF beta 3) and altered responses to the antiproliferative effects of TGF beta. J Clin Endocrinol Metab 86(2), 913–920.10.1210/jcem.86.2.7237. [PubMed: 11158066]

Lewis TD, Malik M, Britten J, San Pablo AM, Catherino WH, 2018. A Comprehensive Review of the Pharmacologic Management of Uterine Leiomyoma. Biomed Res Int 2018, 2414609.10.1155/2018/2414609.

Luo X, Ding L, Xu J, Chegini N, 2005. Gene expression profiling of leiomyoma and myometrial smooth muscle cells in response to transforming growth factor-beta. Endocrinology 146(3), 1097–1118.10.1210/en.2004-1377. [PubMed: 15604209]

Malik M, Catherino WH, 2007. Novel method to characterize primary cultures of leiomyoma and myometrium with the use of confirmatory biomarker gene arrays. Fertil Steril 87(5), 1166–1172.10.1016/j.fertnstert.2006.08.111. [PubMed: 17222838]

Mallikarjuna P, Raviprakash TS, Aripaka K, Ljungberg B, Landstrom M, 2019. Interactions between TGF-beta type I receptor and hypoxia-inducible factor-alpha mediates a synergistic crosstalk leading to poor prognosis for patients with clear cell renal cell carcinoma. Cell Cycle 18(17), 2141–2156.10.1080/15384101.2019.1642069. [PubMed: 31339433]

Massagué J, Wotton D, 2000. Transcriptional control by the TGF-beta/Smad signaling system. Embo j 19(8), 1745–1754.10.1093/emboj/19.8.1745. [PubMed: 10775259]

Mayer A, Höckel M, Wree A, Leo C, Horn LC, Vaupel P, 2008. Lack of hypoxic response in uterine leiomyomas despite severe tissue hypoxia. Cancer Res 68(12), 4719–4726.10.1158/0008-5472.Can-07-6339. [PubMed: 18559518]

McMahon S, Charbonneau M, Grandmont S, Richard DE, Dubois CM, 2006. Transforming growth factor beta1 induces hypoxia-inducible factor-1 stabilization through selective inhibition of PHD2 expression. J Biol Chem 281(34), 24171–24181.10.1074/jbc.M604507200. [PubMed: 16815840]

Moon YM, Kang HJ, Cho JS, Park IH, Lee HM, 2012. Nox4 mediates hypoxia-stimulated myofibroblast differentiation in nasal polyp-derived fibroblasts. Int Arch Allergy Immunol 159(4), 399–409.10.1159/000337658. [PubMed: 22846744]

Nishi H, Nakada T, Hokamura M, Osakabe Y, Itokazu O, Huang LE, Isaka K, 2004. Hypoxia-inducible factor-1 transactivates transforming growth factor-beta3 in trophoblast. Endocrinology 145(9), 4113–4118.10.1210/en.2003-1639. [PubMed: 15155569]

Norian JM, Malik M, Parker CY, Joseph D, Leppert PC, Segars JH, Catherino WH, 2009. Transforming growth factor beta3 regulates the versican variants in the extracellular matrix-rich uterine leiomyomas. Reprod Sci 16(12), 1153–1164.10.1177/1933719109343310. [PubMed: 19700613]

Salama SA, Diaz-Arrastia CR, Kilic GS, Kamel MW, 2012. 2-Methoxyestradiol causes functional repression of transforming growth factor beta3 signaling by ameliorating Smad and non-Smad signaling pathways in immortalized uterine fibroid cells. Fertil Steril 98(1), 178–184.10.1016/j.fertnstert.2012.04.002. [PubMed: 22579131]

Zhang Y, Tang HM, Liu CF, Yuan XF, Wang XY, Ma N, Xu GF, Wang SP, Deng J, Wang X, 2019. TGF-β3 Induces Autophagic Activity by Increasing ROS Generation in a NOX4-Dependent Pathway. Mediators Inflamm 2019, 3153240.10.1155/2019/3153240.

Zhou G, Dada LA, Wu M, Kelly A, Trejo H, Zhou Q, Varga J, Sznajder JI, 2009. Hypoxia-induced alveolar epithelial-mesenchymal transition requires mitochondrial ROS and hypoxia-inducible factor 1. Am J Physiol Lung Cell Mol Physiol 297(6), L1120–1130.10.1152/ajplung.00007.2009. [PubMed: 19801454]

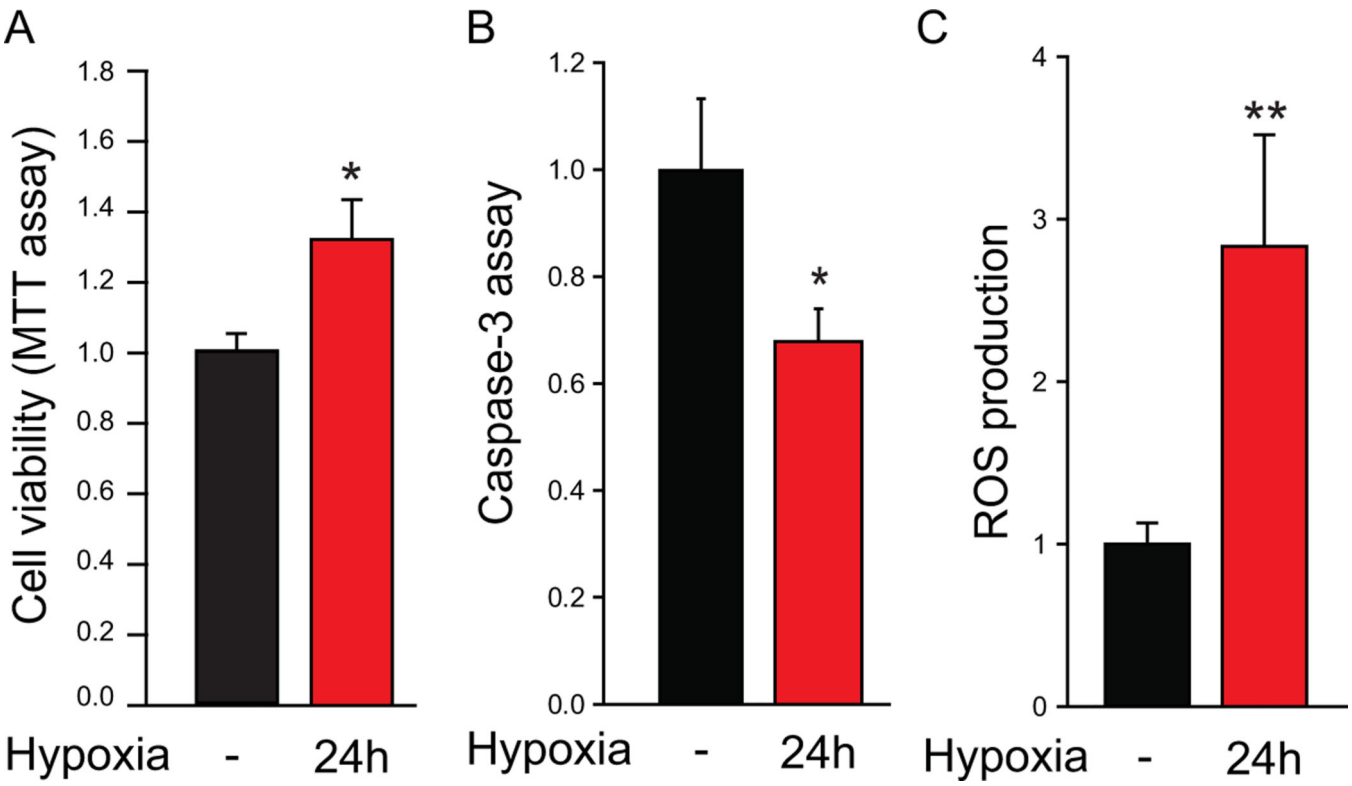

FIGURE 1. Hypoxia induces proliferation and ROS generation and inhibits apoptosis in leiomyoma cells.

Leiomyoma cells were cultured under hypoxic condition (2% O_2) for 24 hours. Cell viability was assayed by using MTT assay (A, n=8). A fluorometric caspase-3 activity assay was performed with cell lysates (B, n=5). ROS generation measured by H2DCFDA (C, n=7). Results are expressed as mean ± SEM. **P*<0.05; ***P*<0.005; normoxia vs hypoxia. ROS, reactive oxygen species; SEM, standard error of the mean.

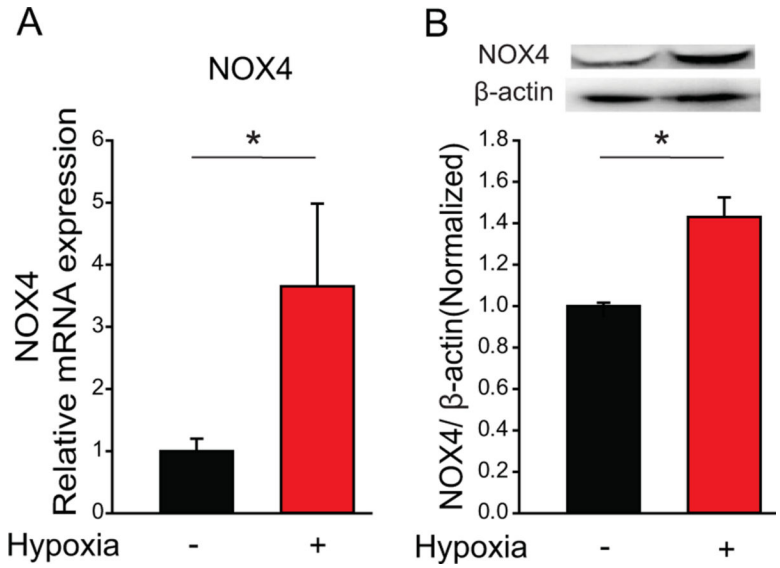

FIGURE 2. Hypoxia induces NOX4 expression.

Leiomyoma cells were cultured under hypoxic condition (2% O_2) for 24 hours. The mRNA levels of *NOX4 ge*nes were measured by qRT-PCR. RPLP0 was amplified under the same qRT-PCR conditions for normalizing quantitative data (A, n=5). The protein level of NOX4 was measured by western blotting and quantified using β-actin as the loading control (B, n=4). Results are expressed as mean± SEM. **P*<0.05; normoxia vs hypoxia. NOX4, nicotinamide adenine dinucleotide phosphate (NADPH) oxidase 4; SEM, standard error of the mean.

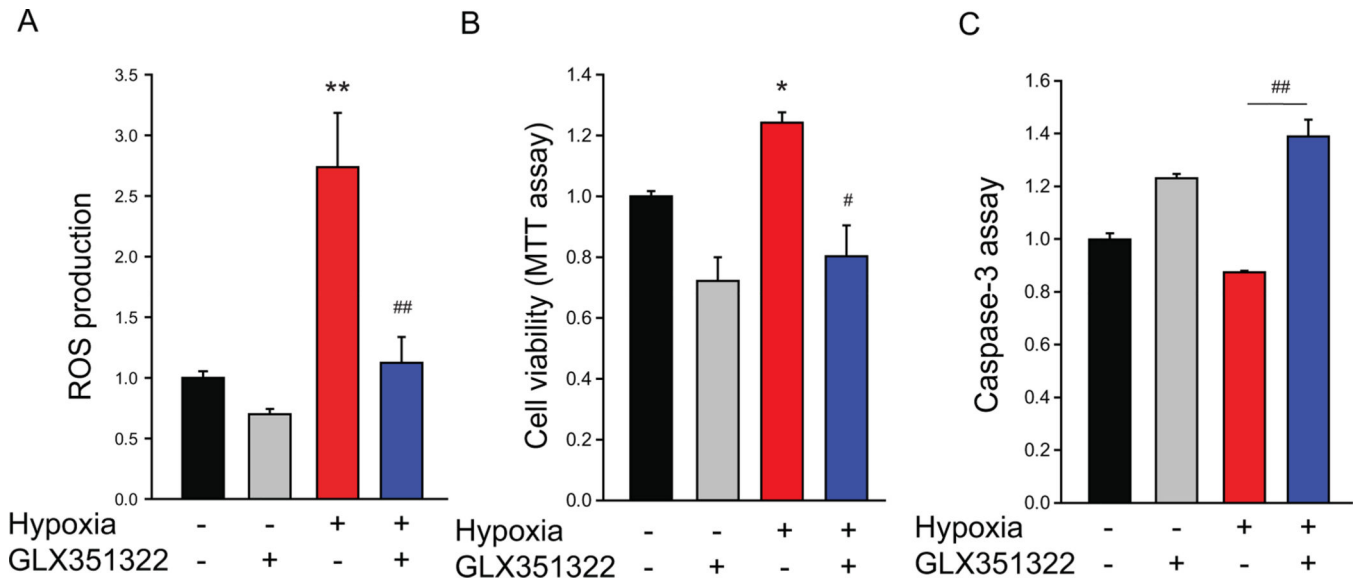

FIGURE 3. NOX4 mediates hypoxia-induced ROS generation and proliferation and apoptosis inhibition in leiomyoma cells.

Leiomyoma cells were cultured under hypoxic condition (2% O_2) with or without GLX351322 (40 μM) for 24 hours. ROS generation measured by H2DCFDA (A, n=4). Cell viability was assayed by using MTT assay (B, n=4). A fluorometric caspase-3 activity assay was performed with cell lysates (C, n=3). Results are expressed as mean ± SEM. *P<0.05, **P<0.005; normoxia vs hypoxia. #P<0.05, ##P<0.005; Hypoxia vs with GLX351322. ROS, reactive oxygen species; SEM, standard error of the mean.

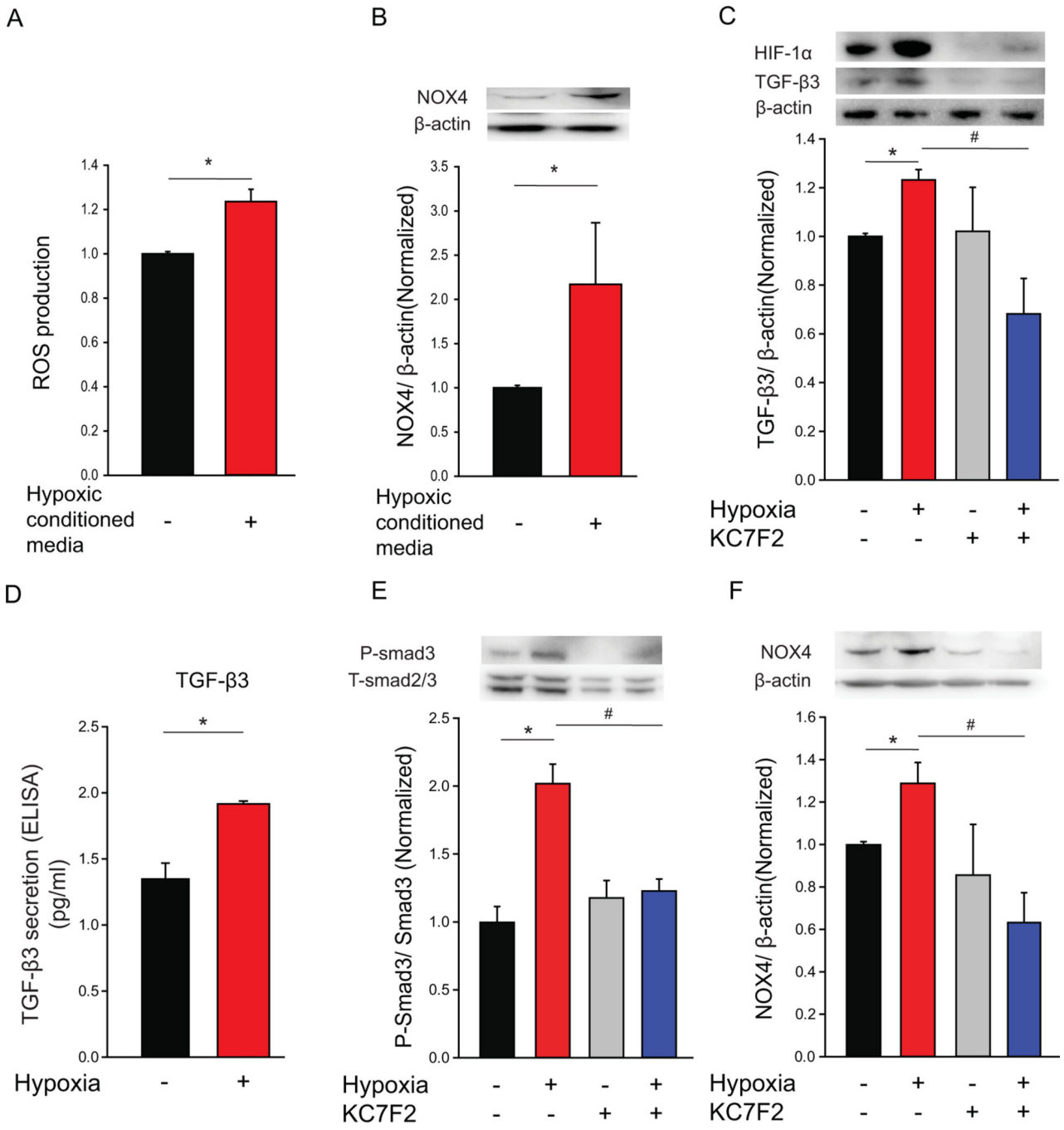

FIGURE 4. Autocrine factors mediating hypoxic NOX4 expression.

(A, B) Leiomyoma cells were treated with hypoxia-preconditioned medium for 24 hours. ROS generation measured by H2DCFDA in hypoxia-preconditioned media and in normoxic media (A, n=4). Western blot for NOX4 protein in hypoxia-preconditioned media and in normoxic media (B, n=4). (C-F) Leiomyoma cells were cultured under hypoxic condition (2% O_2) with or without KC7F2 (20 μM) for 24 hours. The protein levels of HIF-1α and TGF-β3 were measured by western blotting and quantified using β-actin as the loading control (C, n=4). The protein level of TGF-β3 in the culture media measured by ELISA (D,

n=3). The protein levels of phosphorylated Smad3 were measured by western blotting and the data was quantified as the ratio of total Smad3 (E, n=4). The protein level of NOX4 was measured by western blotting and quantified using β-actin as the loading control (F, n=3). Results are expressed as mean ± SEM. *P<0.05; normoxia vs hypoxia; #P<0.05; Hypoxia vs with KC7F2. HIF-1α, hypoxia inducible factor 1 alpha; TGF-β3, transforming growth factor beta 3; NOX4, nicotinamide adenine dinucleotide phosphate (NADPH) oxidase 4; SEM, standard error of the mean.

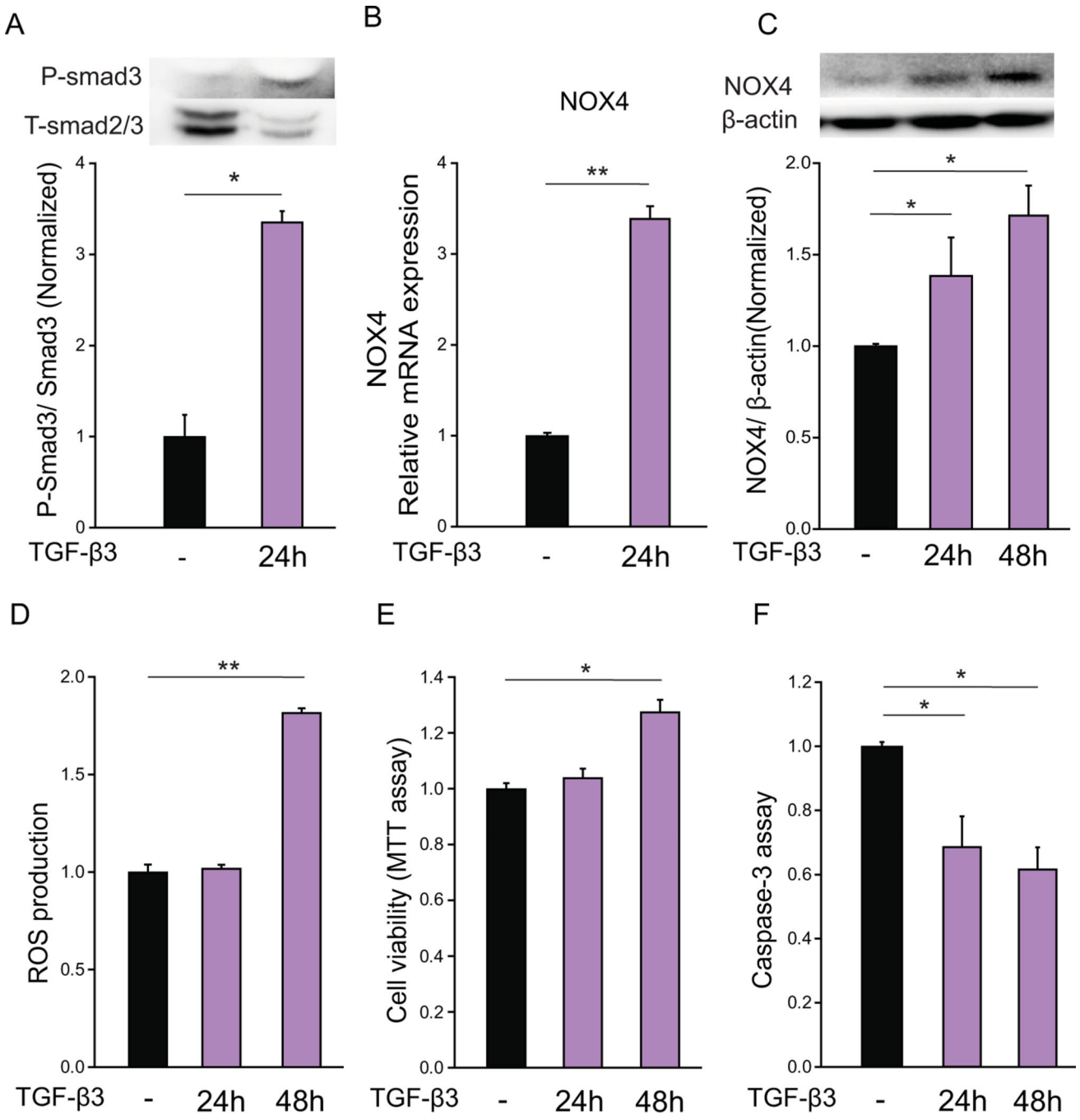

FIGURE 5. TGF-β3 induces NOX4 expression, proliferation and inhibits apoptosis in leiomyoma cells.

Leiomyoma cells were treated with TGF-β3 (10 ng/ml) for 24 or 48 hours. The protein levels of phosphorylated Smad3 were measured by western blotting and the data was quantified as the ratio of total Smad3 (A, n=4).The mRNA levels of *NOX4 ge*nes were measured by qRT-PCR. RPLP0 was amplified under the same qRT-PCR conditions for normalizing quantitative data (B, n=3). The protein level of NOX4 was measured by western blotting and quantified using β-actin as the loading control (C, n=3). ROS generation was measured by H2DCFDA (D, n=3). Cell viability was assayed by using MTT assay (E, n=3).

A fluorometric caspase-3 activity assay was performed with cell lysates (F, n=3). Results are expressed as mean ± SEM. *P<0.05, **P<0.005; vs control.; TGF-β3, transforming growth factor beta 3; NOX4, nicotinamide adenine dinucleotide phosphate (NADPH) oxidase 4; SEM, standard error of the mean.

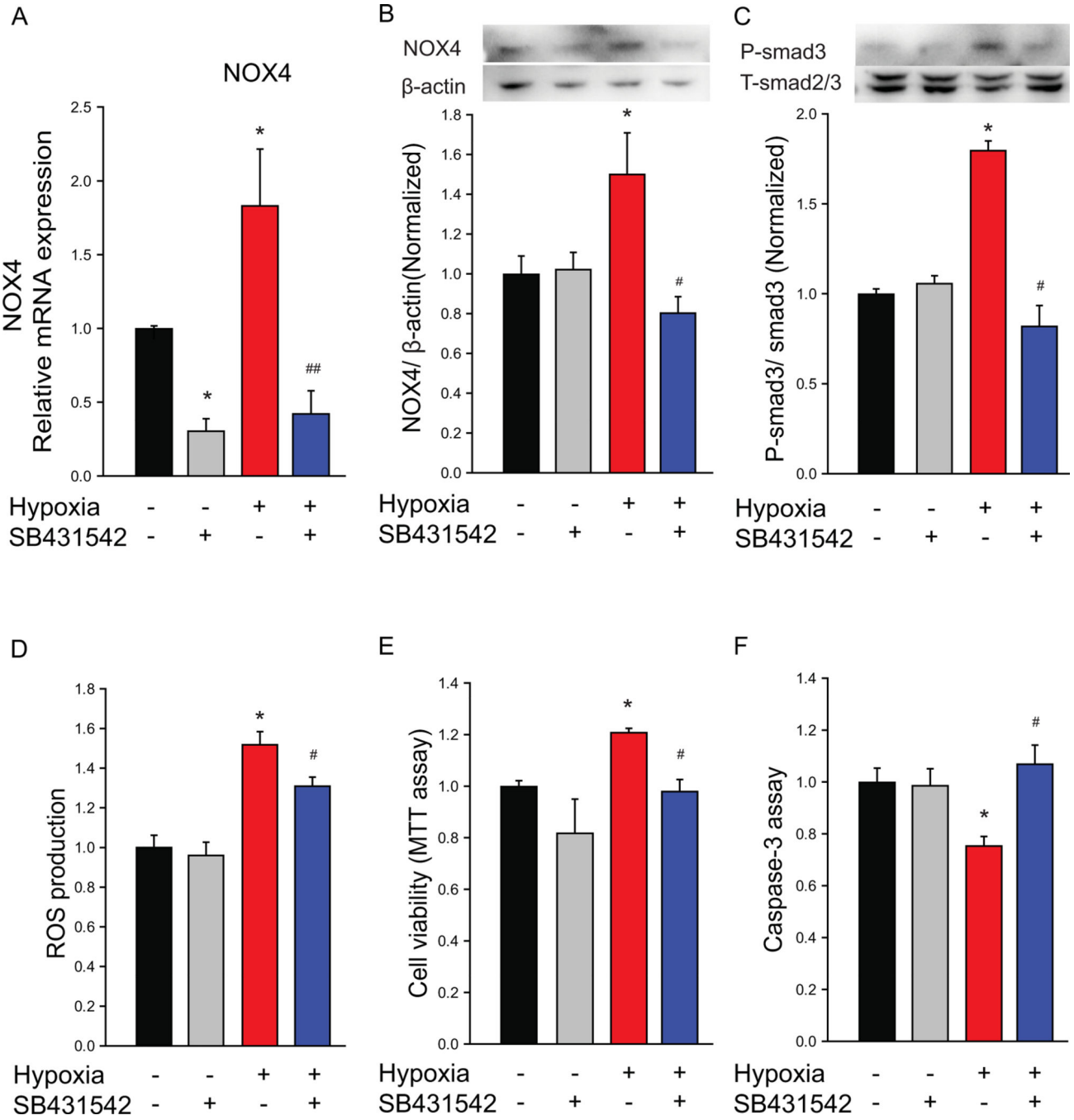

FIGURE 6. TGF-β3 mediates NOX4-dependent hypoxia-induced proliferation, ROS generation and apoptosis inhibition in leiomyoma cells.

Leiomyoma cells were cultured under hypoxic condition (2% O_2) with or without SB431542 (10 μM) for 24 hours. (A) The mRNA levels of *NOX4 ge*nes were measured by qRT-PCR. RPLP0 was amplified under the same qRT-PCR conditions for normalizing quantitative data (n=5). (B) The protein level of NOX4 was measured by western blotting and quantified using β-actin as the loading control (n=3). (C) The protein level of phosphorylated Smad3 were measured by western blotting and the data was quantified as the ratio of total Smad3 (n=3). (D) ROS generation was measured by H2DCFDA (n=3). (E) Cell viability

was assayed by using MTT assay (n=3). (F) A fluorometric caspase-3 activity assay was performed with cell lysates (n=3). Results are expressed as mean ± SEM. *P<0.05; normoxia vs hypoxia. #P<0.05, ##P<0.05; Hypoxia vs with SB431542. NOX4, nicotinamide adenine dinucleotide phosphate (NADPH) oxidase 4; TGF-β3, transforming growth factor beta 3; ROS, reactive oxygen species; SEM, standard error of the mean.